JOURNAL OF BACTERIOLOGY, Aug. 2007, p. 5617–5625 Vol. 189, No. 15
0021-9193/07/$08.00+0 doi:10.1128/JB.00443-07

Dominant Role of the cbb_3 Oxidase in Regulation of Photosynthesis Gene Expression through the PrrBA System in *Rhodobacter sphaeroides* 2.4.1[▽]

Yong-Jin Kim,[1] In-Jeong Ko,[2] Jin-Mok Lee,[1] Ho-Young Kang,[1] Young Min Kim,[3] Samuel Kaplan,[4] and Jeong-Il Oh[1]*

Department of Microbiology, Pusan National University, 609-735 Busan, Korea[1]; Korea Science Academy, 614-822 Busan, Korea[2]; Department of Biology, Yonsei University, 120-749 Seoul, Korea[3]; and Department of Microbiology and Molecular Genetics, University of Texas Health Science Center, 6431 Fannin, Houston, Texas 77030[4]

Received 26 March 2007/Accepted 24 May 2007

In this study, the H303A mutant form of the cbb_3 oxidase (H303A oxidase), which has the H303A mutation in its catalytic subunit (CcoN), was purified from *Rhodobacter sphaeroides*. The H303A oxidase showed the same catalytic activity as did the wild-type form of the oxidase (WT oxidase). The heme contents of the mutant and WT forms of the cbb_3 oxidase were also comparable. However, the *puf* and *puc* operons, which are under the control of the PrrBA two-component system, were shown to be derepressed aerobically in the *R. sphaeroides* strain expressing the H303A oxidase. Since the strain harboring the H303A oxidase exhibited the same cytochrome *c* oxidase activity as the stain harboring the WT oxidase did, the aerobic derepression of photosynthesis gene expression observed in the H303A mutant appears to be the result of a defective signaling function of the H303A oxidase rather than reflecting any redox changes in the ubiquinone/ubiquinol pool. It was also demonstrated that ubiquinone inhibits not only the autokinase activity of full-length PrrB but also that of the truncated form of PrrB lacking its transmembrane domain, including the proposed quinone binding sequence. These results imply that the suggested ubiquinone binding site within the PrrB transmembrane domain is not necessary for the inhibition of PrrB kinase activity by ubiquinone. Instead, it is probable that signaling through H303 of the CcoN subunit of the cbb_3 oxidase is part of the pathway through which the cbb_3 oxidase affects the relative kinase/phosphatase activity of the membrane-bound PrrB.

Rhodobacter sphaeroides, a nonsulfur photosynthetic bacterium, is a model organism that has been extensively studied with respect to redox-sensing mechanisms and the control of gene expression. *R. sphaeroides* can grow both aerobically and anaerobically, and an array of diverse cellular processes, such as photosynthesis, respiration, CO_2 fixation, and N_2 fixation, have been shown to be controlled in response to changes in environmental oxygen tension and light intensity (3, 10, 11, 17, 23, 34, 35). These environmental parameters directly influence the cellular redox state. *R. sphaeroides* is capable of performing photosynthesis (PS) anaerobically in the presence of light. When oxygen tensions fall below ~3%, expression of the PS genes encoding the apoproteins of the photosynthetic apparatus as well as enzymes catalyzing the biosynthesis of the photopigments (bacteriochlorophyll and carotenoid) is induced (13, 23). The PrrBA two-component regulatory system has been shown to play a pivotal role in the induction of the PS genes in response to changes in oxygen tension (4–6, 11).

The PrrBA two-component system comprises the membrane-associated PrrB histidine kinase and its cognate PrrA response regulator (4–6). PrrB is composed of the conserved C-terminal kinase/phosphatase domain and the N-terminal transmembrane domain with six transmembrane helices forming three periplasmic and two cytoplasmic loops (28). The PrrB histidine kinase is a bifunctional enzyme that possesses both kinase and phosphatase activities acting on PrrA (1, 27, 33). Oh et al. proposed that the central portion of the PrrB transmembrane domain, including the second periplasmic domain, plays an important role in the sensory function of PrrB and that the default state of PrrB activity is in the kinase-dominant mode (26).

Three models have been proposed to explain the mechanisms by which the PrrB histidine kinase perceives oxygen tension. The first model proposed by Oh and Kaplan contends that the cbb_3 cytochrome *c* oxidase of the respiratory electron transport chain (ETC) serves as both redox sensor and modulator of PrrB kinase/phosphatase activity (25). According to this model, the cbb_3 oxidase generates an "inhibitory" signal that shifts the relative equilibrium of PrrB activity from the kinase mode to the phosphatase-dominant mode under conditions of high oxygen by increasing the phosphatase activity of PrrB without alteration of the PrrB kinase activity (27). This results in the silencing of PS gene expression. Under anaerobic or oxygen-limiting conditions, the inhibitory signal emanating from the cbb_3 oxidase is weakened and thereby the relative activity of PrrB is in its default state, i.e., the kinase-dominant mode. Another model was proposed from the study of RegB (a close homolog of PrrB from *Rhodobacter capsulatus*), which suggests that the redox state of the membrane-localized ubiquinone/ubiquinol pool of the ETC controls the kinase activity of RegB (39). The binding of oxidized ubiquinone to the GGXXNPF motif conserved at the junction of the second

* Corresponding author. Mailing address: Department of Microbiology, Pusan National University, 30 Jangjeon-dong, Geumjeong-gu, 609-735 Busan, Korea. Phone: 82-51-510-2593. Fax: 82-51-514-1778. E-mail: joh@pusan.ac.kr.

▽ Published ahead of print on 8 June 2007.

TABLE 1. Bacterial strains and plasmids used in this study

Strain or plasmid	Relevant phenotype or genotype	Source or reference
Strains		
E. coli		
DH5α	(ϕ80d*lacZ*Δ*M15*) Δ*lacU169 recZ1 endA1 hsdR17 supE44thi1 gyrA96 relA1*	9
Bl21(DE3)	F^- *ompT* $hsdS_B$ (r_B^- m_B^-) *dcm gal* λ(DE3)	Promega
S17-1	Pro^- Res^- Mob^+ *recA*; integrated plasmid RP4-Tc::Mu-Km::Tn*7*	38
R. sphaeroides		
2.4.1	WT	42
CBB3Δ	2.4.1 Derivative, deletion of *ccoNOQP*	24
PRRB1	2.4.1 Derivative, Δ*prrB*::Ω Sp^r/St^r	5
Plasmids		
pCCO2	pUC19::4.7-kb BamHI-EcoRI fragment containing *ccoNOQP*	25
pCCO2H303A	pCCO2 in which the codon for H303 is displaced with GCC	21
pCCO2H303ANHIS	pCCO2H303A in which *ccoN* contains six histidine codons before its stop codon	This study
pRK415	Tc^r; Mob^+ *lacZ*α IncP	12
pUI2803NHIS	pRK415::4.7-kb BamHI-EcoRI fragment containing *ccoNOQP* in which *ccoN* contains six histidine codons before its stop codon	24
pUIH303A	pUI2803NHIS in which the codon for H303 is displaced with GCC	This study
pUI1663	Sp^r St^r Km^r; IncQ, *puf*::*lacZYA′*	4
pCF200Km	Sp^r St^r Km^r; IncQ, *puf*::*lacZYA′*	18
pPRRB4	pRK415::1.6-kb PstI-KpnI fragment containing *prr*B from pPRRB3; *prr*B is in colinear orientation to *lacZ*	26
pPRRB4Q93N	pPRRB4 in which the codon for Q93 is displaced with AAC	14
pT7HIS9A	pT7-7::1.4-kb NdeI-PstI fragment containing *prrB* with nine His codons before its stop codon	27
pT7HIS9C	pT7-7::0.9-kb NdeI-PstI fragment containing the 3′-part of *prrB* with nine His codons before its stop codon	27
pT7Q93N	pT7HIS9A in which the codon for Q93 is displaced with AAC	This study

periplasmic loop and the fourth transmembrane helix of the RegB transmembrane domain was shown to inhibit RegB kinase activity, whereas reduced ubiquinol did not affect RegB kinase activity (39). Since the redox balance of the ubiquinone/ubiquinol pool is known to shift to the oxidized state in a *Rhodobacter* strain grown under aerobic conditions (30), this model can account for aerobic repression of the genes belonging to the RegA regulon. The last model, also suggested by Swem et al. for redox sensing by RegB, is that the conserved cysteine (C265 of RegB) functions as a redox switch that controls RegB kinase activity through a metal-dependent, more specifically Cu^{2+}, formation of a disulfide bond in response to redox changes (40). Under oxidizing conditions, RegB forms a quaternary structure of homotetramer through disulfide bond formation between the RegB dimers, which leads to the inactivation of RegB kinase activity.

The catalytic subunit (CcoN) of the *R. sphaeroides* cbb_3 oxidase contains five histidine residues (H214, H233, H303, H320, and H444) that are conserved in most CcoN subunits of the cbb_3 oxidase but not in the catalytic subunits of other members of the copper-heme superfamily oxidases (21, 41). It was demonstrated in vivo that the H320A mutation leads to an almost complete loss of cbb_3 oxidase activity, whereas the H214A mutation does not affect the catalytic ability of the cbb_3 oxidase to reduce O_2 to H_2O using electrons derived from reduced cytochrome *c* (21). The H233V and H444A mutations result in a partial loss of cbb_3 oxidase activity. Interestingly, the *R. sphaeroides* mutant strain synthesizing the H303A mutant form of the cbb_3 oxidase (H303A oxidase) retains cytochrome *c* oxidase activity similar to that detected in the *R. sphaeroides* expressing the wild-type form of the cbb_3 oxidase (WT oxidase), but aberrantly synthesizes spectral complexes under aerobic conditions (21). In this study, we characterized in detail the *R. sphaeroides* mutant strain synthesizing the H303A oxidase. The purified H303A oxidase has the same catalytic activity and heme content as the WT oxidase, but is defective in generation of the signal to turn off the expression of PS genes in the presence of O_2. We also provide evidence that ubiquinone inhibits not only autophosphorylation of full-length PrrB but also that of the truncated PrrB lacking its transmembrane domain and its presumed ubiquinone binding sequence. These findings and others imply that the suggested ubiquinone binding site within the PrrB transmembrane domain is not required for the inhibition of PrrB kinase activity by ubiquinone. Instead, the case for a direct interaction between the cbb_3 oxidase and PrrB is strengthened.

MATERIALS AND METHODS

Bacterial strains, plasmids, and culture conditions. The bacterial strains and plasmids used in this study are listed in Table 1. *R. sphaeroides* and *Escherichia coli* strains were grown on Sistrom's medium A (SIS) and Luria-Bertani (LB) medium, respectively, as described previously (22), except that chemoheterotrophic cultures of *R. sphaeroides* were grown aerobically by sparging with ambient air.

DNA manipulations and conjugation techniques. Standard protocols or manufacturer's instructions were followed for recombinant DNA manipulations (36). The mobilization of plasmids from *E. coli* strains into *R. sphaeroides* strains was carried out as described elsewhere (2).

Construction of plasmids. For the construction of pUIH303A, a 0.8-kb ApaI fragment containing the 3′ portion of *ccoN* with a tail of six histidine codons immediately upstream of its stop codon from pUI2803NHIS was cloned into pCCO2H303A digested by ApaI, replacing the 0.8-kb WT ApaI fragment. The resulting plasmid, pCCO2H303ANHIS, with the correct orientation of the 0.8-kb ApaI fragment was digested with BamHI and EcoRI, and a 4.7-kb BamHI-

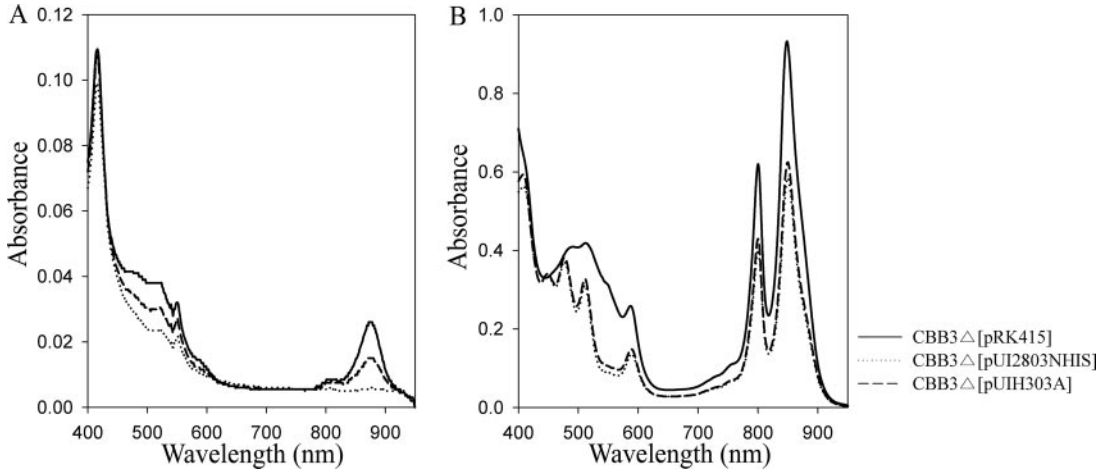

FIG. 1. Spectral complex formation in the *R. sphaeroides* strain expressing the His_6-tagged H303A oxidase. The CBB3Δ strains carrying the corresponding plasmids were grown either aerobically by sparging with ambient air to an optical density at 600 nm of 0.4 to 0.5 (A) or anaerobically with DMSO in the dark for 5 days (B). The CBB3Δ strains containing pRK415 and pUI2803NHIS were used in these experiments as control strains. Seven hundred micrograms of the crude extracts were used to record the spectra between 400 and 950 nm. The peak or shoulder at 875 indicates the B875 complex (light harvesting complex I). The peaks at 800 and 850 represent the B800-B850 complex (light harvesting complex II).

EcoRI fragment was ultimately cloned into pRK415, which was restricted with the same enzymes, giving plasmid pUIH303A.

Plasmid pT7Q93N was constructed to heterologously express the mutant form (Q93N) of PrrB by site-directed mutagenesis using the *prrB* expression plasmid pT7HIS9A. Mutagenesis was carried out using the QuikChange site-directed mutagenesis kit (Stratagene, La Jolla, CA). Mutations were verified by DNA sequencing.

Protein purification. The His-tagged PrrB, C-PrrB (a truncated form of PrrB in which the 191 N-terminal amino acids are removed), and cbb_3 cytochrome *c* oxidase were purified as described previously (24, 27).

In vitro phosphorylation assay. Protein phosphorylation was performed at 30°C in assay buffer containing the appropriate protein components, 20 mM Tris-HCl (pH 8.0), 50 mM KCl, 5 mM $MgCl_2$, 10 to 15% (wt/vol) glycerol, 10 mM β-mercaptoethanol, and 0.025% (wt/vol) *n*-dodecyl β-D-maltoside. For autophosphorylation assays of PrrB, an appropriate amount of PrrB was incubated in assay buffer in the presence or absence of oxidized/reduced coenzyme Q1 (Sigma, St. Louis, MO) for 20 min at 30°C and the reaction was initiated by the addition of a mixture of [γ-^{32}P]ATP and unlabeled ATP to a final concentration of 100 μM (1,000 Ci/mole). For time course experiments, samples (10 μl) were removed at various time intervals and reactions were stopped by the addition of 3 μl of 4× loading buffer (40 mM Tris-HCl [pH 6.8], 4% [wt/vol] sodium dodecyl sulfate [SDS], 16% [wt/vol] glycerol, 16 mM dithiothreitol [DTT], 1% [vol/vol] β-mercaptoethanol, 0.1% [wt/vol] bromophenol blue, and 100 mM EDTA). Coenzyme Q_1 was dissolved in 95% ethanol at a concentration of 12.5 mM as a 50× stock solution. The 50× stock solution of coenzyme Q_1 was added to the assay mixture to a final concentration of 250 μM (for the negative control experiment, the same volume of 95% ethanol was added to the assay mixture). For the reduction of coenzyme Q1 (ubiquinone) to ubiquinol, DTT was added to both the ubiquinone stock solution and the phosphorylation assay mixture to a final concentration of 10 mM. Samples were denatured for 40 min at room temperature in loading buffer, and ^{32}P-labeled PrrB was resolved by SDS-polyacrylamide gel electrophoresis (PAGE) using 12.5% (wt/vol) polyacrylamide gels. Gels were dried at 80°C under vacuum, and the labeled proteins were visualized by autoradiography. The dried gel was autoradiographed with an X-ray film (BioMax XAR film; Kodak, Rochester, NY) in an exposure cassette at −70°C for 1 to 3 days.

Spectroscopic and immunoblotting analyses. Dithionite-reduced minus air-oxidized spectra were obtained by procedures as described previously (25). The levels of the B800-B850 and B875 complexes were determined spectrophotometrically as described previously (22). SDS-PAGE and Western blotting analyses were performed as described elsewhere (16, 19). Quantitation of the band intensity of CcoN and CcoO subunits was performed with a densitometer program, ImageJ, version 1.37.

Enzyme assays, protein determination, and heme staining. Preparation of crude extracts and determination of β-galactosidase activities were performed as described previously (22). Cytochrome *c* oxidase activities were measured spectrophotometrically with reduced horse heart cytochrome *c* (Sigma) as previously described elsewhere (22). Protein concentration was determined by the Bio-Rad protein assay kit (Bio-Rad, Hercules, CA) with bovine serum albumin as the standard protein. Heme staining was performed using 3,3′,5,5′-tetramethyl benzidine (Sigma) and H_2O_2 as described previously (24).

RNA isolation and reverse transcription-PCR (RT-PCR). Total RNA was isolated from *R. sphaeroides* strains using TRIzol reagent as instructed by the manufacturer (Invitrogen, Carlsbad, CA). The first-strand cDNA was synthesized from 5 μg of total RNA by using a BD Sprint PowerScript single shots kit (Clontech, Mountain View, CA). Two micrograms of the first-strand reaction mixture was used as a template for PCR, and 15 cycles of PCR were performed. PCR products were analyzed by electrophoresis on a 2% (wt/vol) agarose gel. To amplify internal portions of the *pufB* and 16S rRNA genes, the following oligonucleotides were used: pufBF (5′-GGCTGATAAATCCGACCTGGG-3′) and pufBR (5′-GAACCACGGACGCCAGATGT-3′) for the *pufB* gene and rsp42F (5′-CGGATCGGAAAGTCAGAGG-3′) and rsp42R (5′-CAGCGTCAGTATC GAGCCAG-3′) for the 16S rRNA gene.

RESULTS

In vivo characterization of the His_6-tagged H303A mutant form of the cbb_3 oxidase in *R. sphaeroides*. In order to purify and characterize the H303A oxidase from *R. sphaeroides*, we constructed the plasmid pUIH303A in which the *ccoNOQP* operon with the H303A mutation and a tail of six histidine codons immediately prior to the *ccoN* stop codon is cloned into pRK415. The plasmid was introduced into the *R. sphaeroides* CBB3Δ strain in which the entire *ccoNOQP* operon is deleted. When grown aerobically on Sistrom's medium A agar plates, the CBB3Δ strain carrying pUIH303A (CBB3Δ [pUIH303A]) formed colonies with red pigmentation compared with the relatively pale pink coloration of the control strain CBB3Δ containing pUI2803NHIS that has no mutation at position H303 and is otherwise the same construct as pUIH303A. To determine the levels of spectral complexes, spectra were recorded from crude extracts of CBB3Δ [pUIH303A] as well as from the control strains, CBB3Δ [pUI2803NHIS] and CBB3Δ [pRK415] (Fig. 1). When grown under aerobic conditions, CBB3Δ [pUIH303A] synthesized an intermediate level of the

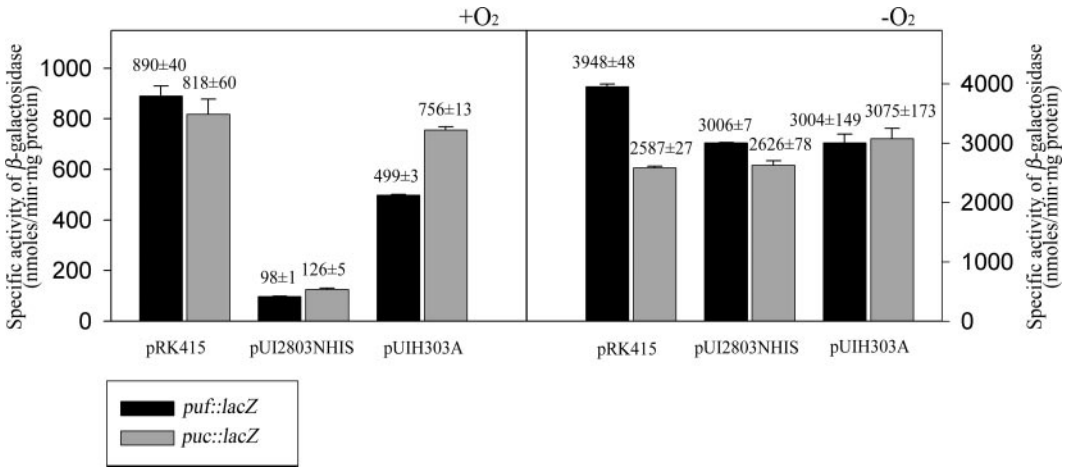

FIG. 2. Expression of the *puf* and *puc* operons in *R. sphaeroides* CBB3Δ. Strains bearing the *puf*::*lacZ* or *puc*::*lacZ* transcriptional fusion plasmid were grown either aerobically ($+O_2$) or anaerobically ($-O_2$) as described for Fig. 1. β-galactosidase activities are indicated. All values provided are the averages of two independent determinations. Error bars indicate standard deviations.

B875 complex that was 41% of that observed for CBB3Δ [pRK415] producing no cbb_3 oxidase, whereas the positive control strain CBB3Δ [pUI2803NHIS] producing the WT oxidase did not produce any spectral complexes. When grown under anaerobic conditions with dimethyl sulfoxide (DMSO) as a terminal electron acceptor, spectral complex formation was strongly induced in all these strains (Fig. 1B). The levels of spectral complexes (B800-B850 and B875) synthesized in CBB3Δ [pUIH303A] were virtually the same as those in CBB3Δ [pUI2803NHIS]. The negative control strain CBB3Δ [pRK415] produced 1.5- and 1.6-fold higher amounts of the B800-B850 and B875 complexes, respectively, than the other two strains, which is consistent with previous observations that inactivation of the cbb_3 oxidase leads to synthesis of elevated levels of the spectral complexes in *R. sphaeroides* grown anaerobically (20).

Using *puf*::*lacZ* and *puc*::*lacZ* transcriptional fusions, we next investigated the expression levels of the *puf* and *puc* operons that encode the apoproteins of the spectral complexes and are known to be regulated by the PrrBA two-component system. As shown in Fig. 2, only basal expression levels of the *puf* operon were observed in CBB3Δ [pUI2803NHIS] strains grown aerobically, whereas expression of the *puf* operon was increased in CBB3Δ [pUIH303A] grown aerobically by a factor of 5.1 compared with CBB3Δ [pUI2803NHIS] grown under the same conditions. When grown under anaerobic dark-DMSO conditions, the expression of the *puf* operon was strongly induced in all these strains. The expression of *puf* in CBB3Δ [pUIH303A] was induced to a level comparable to that of CBB3Δ [pUI2803NHIS] but somewhat lower than that observed for the negative control strain CBB3Δ [pRK415]. The expression of the *puc* operon showed a pattern of expression similar to that of the *puf* operon, i.e., aerobic derepression of *puc* in CBB3Δ [pUIH303A]. Taken together, the results from Fig. 1 and Fig. 2 reveal that the PS genes under the control of the PrrBA two-component system are derepressed in a *R. sphaeroides* strain synthesizing the altered H303A oxidase, resulting in "oxygen-insensitive formation of the spectral complexes."

From the results described above, the question arises as to how oxygen-insensitive formation of the spectral complexes and aerobic derepression of PS genes occur in CBB3Δ [pUIH303A]. One possibility is that the H303A oxidase is defective in its catalytic function to reduce O_2 to H_2O by using electrons from reduced cytochromes *c*, which somehow shifts the redox state of the ubiquinone/ubiquinol pool of the ETC to a more reduced state under aerobic conditions. To investigate this possibility, cytochrome *c* oxidase activities were determined in CBB3Δ [pUIH303A] as well as the control strains. When grown under anaerobic dark-DMSO conditions where the cbb_3 cytochrome *c* oxidase is known to be the exclusive cytochrome *c* oxidase synthesized in *R. sphaeroides* (25), CBB3Δ [pUIH303A] exhibited the same cytochrome *c* oxidase activity as did CBB3Δ [pUI2803NHIS] (Fig. 3A). As expected, no cytochrome *c* oxidase activity was detected in the negative control strain CBB3Δ [pRK415] grown under the same conditions. Immunoblotting assays showed that the membrane fractions of the CBB3Δ [pUIH303A] and CBB3Δ [pUI2803NHIS] contained similar levels of the CcoN and CcoP subunits, whereas these same subunits were not detected in the negative control strain CBB3Δ [pRK415]. These results indicate that the H303A oxidase is correctly assembled in the membrane under anaerobic growth conditions and forms a fully functional complex. We next examined cytochrome *c* oxidase activities in *R. sphaeroides* strains grown under aerobic conditions (Fig. 3B). Both CBB3Δ [pUIH303A] and CBB3Δ [pUI2803NHIS] displayed higher cytochrome *c* oxidase activities than did CBB3Δ [pRK415], and the levels of these activities were comparable. The cytochrome *c* oxidase activity detected in CBB3Δ [pRK415] is due to the presence of the aa_3 cytochrome *c* oxidase. The levels of the CcoN and CcoP subunits in the membrane fractions of CBB3Δ [pUIH303A] grown under aerobic conditions were similar to those observed for CBB3Δ [pUI2803NHIS] grown under the same conditions. Taken together, the results from Fig. 3 indicate that the H303A mutation affects neither the catalytic activity of the cbb_3 oxidase in *R. sphaeroides* nor its assembly into the membrane in *R. sphaeroides* grown under aerobic and anaerobic conditions.

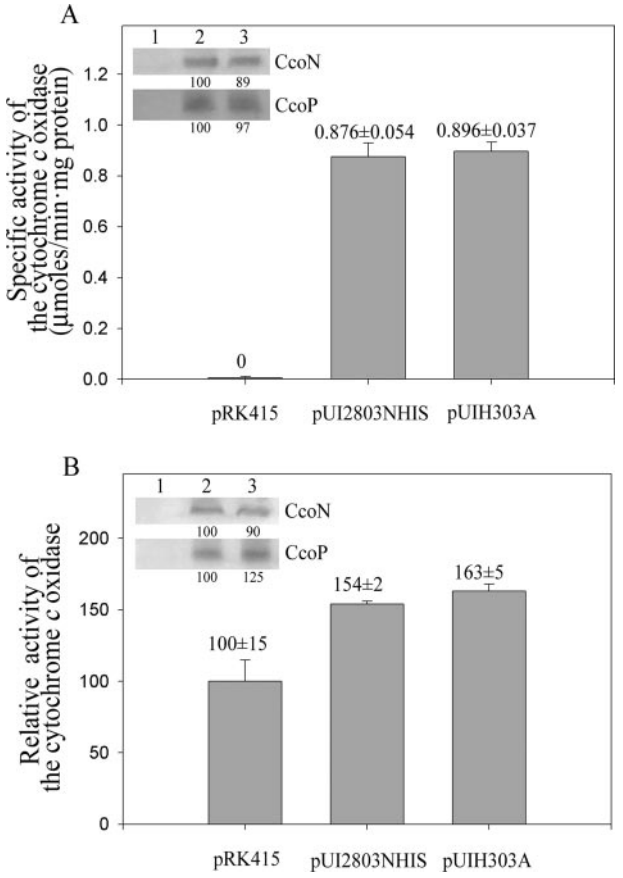

FIG. 3. Determination of cytochrome *c* oxidase activities and immunoblot analysis for the detection of the cbb_3 oxidase in *R. sphaeroides* strains. The CBB3Δ strains carrying the corresponding plasmids were grown anaerobically (A) or aerobically (B) as described for Fig. 1. The cbb_3 oxidase activites in the crude extracts were measured spectrophotometrically using reduced horse heart cytochrome *c*, and all values provided are the averages of two independent determinations. For the cytochrome *c* oxidase activites from strains grown aerobically, the activity detected in CBB3Δ [pRK415] is set at 100 and the relative activities are expressed for the other strains. Solubilized membrane proteins (30 μg) isolated from each of the strains were used for Western blotting analysis (inset). The CcoN polypeptide was detected using the anti-His_4 monoclonal antibody (QIAGEN, Valencia, CA), and the CcoP polypeptide was detected by using the polyclonal antibody raised against the CcoP subunit of *R. capsulatus*. Lanes 1, CBB3Δ [pRK415]; 2, CBB3Δ [pUI2803NHIS]; 3, CBB3Δ [pUIH303A]. The relative amounts of CcoP and CcoO are given below the Western blots. Error bars indicate standard deviations.

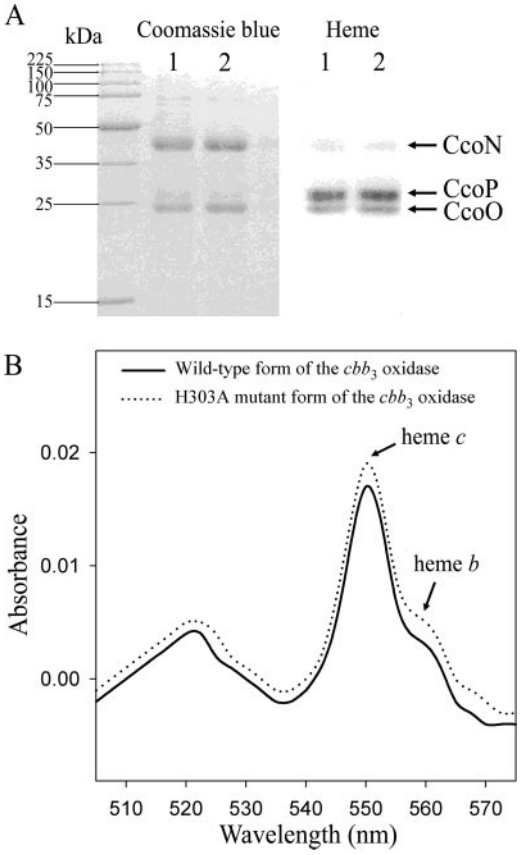

FIG. 4. Comparison of the heme contents between the purified H303A and WT oxidases. (A) Three micrograms each of the purified cbb_3 oxidases from the CBB3Δ [pUI2803NHIS] (lane 1) and the CBB3Δ [pUIH303A] (lane 2) grown under anaerobic dark DMSO conditions was used for SDS-PAGE. Following SDS-PAGE, the gel was vertically cut into two slices containing the same samples. One gel slice was stained with Coomassie brilliant blue and the other was heme stained with 3,3′,5,5′-tetramethyl benzidine and H_2O_2. (B) Dithionite-reduced minus air-oxidized difference spectra between 500 and 600 nm was recorded at room temperature. Seventy micrograms each of the purified cbb_3 oxidases was used for the analysis. The 551- and 561-nm peaks represent *c*-type and *b*-type hemes, respectively.

The purified H303A oxidase has the same heme content and cytochrome *c* oxidase activity as the purified WT oxidase. The H303A and WT oxidases were purified from anaerobically grown CBB3Δ carrying pUIH303A and pUI2803NHIS, respectively, as described in Materials and Methods. As shown in Fig. 4A, two distinct bands of apparent molecular masses of 45 and 24 kDa, which correspond to the CcoN and CcoO subunits of the cbb_3 oxidase, respectively, were clearly visible in the SDS-PAGE gel stained with Coomassie brilliant blue. When the same amounts of the purified H303A and WT oxidases were applied to SDS-PAGE, the band intensities of CcoN and CcoO of the H303A oxidase appeared to be the same as that of the WT oxidase. As reported previously (24), the CcoP band is less well stained with Coomassie brilliant blue compared with other subunit bands. To compare the heme content of each subunit of each form of the oxidase, heme staining was performed and difference spectra were recorded employing the purified cbb_3 oxidases. Heme staining showed that the band intensities of CcoO and CcoP, which are monoheme and diheme cytochromes *c*, respectively, were indistinguishable between the H303A and WT oxidases (Fig. 4A). Although CcoN with noncovalently bound *b*-type hemes was not well stained by heme staining, the CcoN band of the H303A oxidase showed the same intensity as that of the WT oxidase. To more precisely compare the heme content of the purified cbb_3 oxidases, dithionite-reduced minus air-oxidized difference spectra were recorded using the purified oxidases (Fig. 4B). Difference spectra corroborated the fact that the H303A and WT oxidases contain very similar levels of *b*- and *c*-type hemes.

In 20 mM potassium phosphate buffer (pH 7.5) at 30°C, the H303A and WT oxidases exhibited virtually the same K_m val-

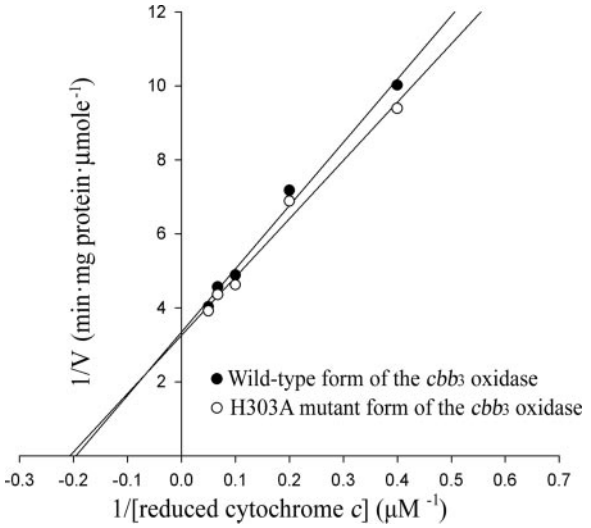

FIG. 5. Lineweaver-Burk plot for the enzymatic kinetics of the purified cbb_3 oxidases. The cbb_3 oxidase activity for reduced horse heart cytochrome *c* was measured spectrophotometrically with varying concentrations of the substrate, reduced cytochrome *c* (2.5, 5, 10, 15, and 20 μM). The results are plotted as 1/enzyme activity versus 1/[substrate]. The apparent values for the K_m of WT and H303A oxidases are 5.1 and 4.9 μM, respectively. The V_{max} values of both enzymes are 0.3 μmol/min · mg protein. V, initial velocity.

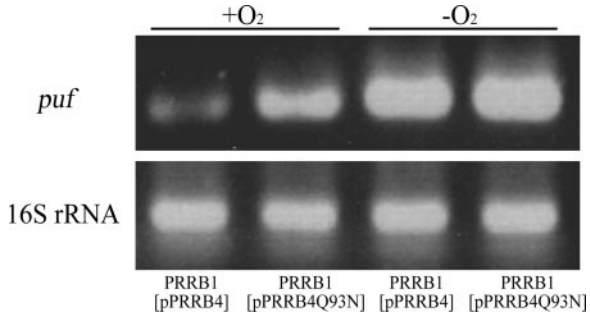

FIG. 6. Effect of the Q93N mutation of PrrB on *puf* expression. *R. sphaeroides* PRRB1 strains carrying pPRRB4 or pPRRB4Q93N were grown aerobically or anaerobically (under dark-DMSO conditions) as described for Fig. 1. Expression of the *puf* operon was analyzed by RT-PCR as described in Materials and Methods. Total RNA was isolated from aerobically ($+O_2$) or anaerobically ($-O_2$) grown *R. sphaeroides* PRRB1 strains carrying the corresponding plasmids, and cDNA was synthesized from 5 μg of total RNA. The PCR products were loaded onto a 2% (wt/vol) agarose gel, yielding 145-bp and 173-bp bands for *pufB* and the 16S rRNA gene, respectively.

ues (4.9 and 5.1 μM, respectively) for reduced horse heart cytochrome *c*, indicating that both the purified oxidases have the same binding affinity for reduced cytochrome *c* (Fig. 5). The V_{max} values of the H303A and WT oxidases were also identical (0.3 μmol/min · mg protein) when saturating levels of reduced cytochrome *c* were present in the assay mixture.

The proposed ubiquinone binding site of PrrB is not required for the inhibition of PrrB autophosphorylation by ubiquinone. Site-directed mutagenesis of the conserved amino acids in the second periplasmic loop of the PrrB transmembrane domain revealed that D90, Q93, L94, L98, and N106 might be involved in this redox sensory activity (14). Mutations of D90N, Q93N, L94C, and L98C led to constitutive formation of the spectral complexes in *R. sphaeroides* regardless of the presence or absence of O_2. The *R. sphaeroides* strains synthesizing the Q93A, N106A, and N106Q mutant forms of PrrB were shown to be unstable (forming colonies with variegated colorization and size) under aerobic growth conditions, most likely due to high levels of PS gene expression in these mutant strains even under aerobic conditions. Among the phenotypically stable *R. sphaeroides* strains synthesizing the mutant forms of PrrB, the Q93N mutant of *R. sphaeroides* produced the highest levels of spectral complexes under aerobic conditions (14). The *R. sphaeroides* PRRB1 strain carrying pPRRB4Q93N (PRRB1 [pPRRB4Q93N]) synthesizes the Q93N mutant form of PrrB (Q93N PrrB). When grown aerobically, the PRRB1 [pPRRB4Q93N] strain synthesized 6.4- and 8.1-fold increased levels of the B800-B850 and B875 complexes, respectively, compared with the PRRB1 strain synthesizing the WT form of PrrB (PRRB1 [pPRRB4]) (data not shown). Under anaerobic dark-DMSO conditions, the levels of the spectral complexes synthesized in PRRB1 [pPRRB4Q93N] were 2.3-fold higher than those detected for pPRRB1 [pPRRB4] (data not shown). By means of RT-PCR, the expression level of the *pufB* gene was determined in the PRRB1 [pPRRB4Q93N] as well as in the control strain PRRB1 [pPRRB4]. As shown in Fig. 6, the expression of *pufB* was significantly derepressed in PRRB1 [pPRRB4Q93N] grown under aerobic conditions compared with PRRB1 [pPRRB4] grown under the same conditions. This result is consistent with the levels of spectral complex formation in PRRB1 [pPRRB4Q93N] grown under aerobic conditions. When the *R. sphaeroides* strains were grown under anaerobic dark-DMSO conditions, *pufB* was highly expressed in both strains and its expression levels in PRRB1 [pPRRB4Q93N] were slightly higher than those observed for PRRB1 [pPRRB4]. A plausible explanation for spectral complex formation and derepression of PS gene expression in the PRRB1 [pPRRB4Q93N] strain grown aerobically is that Q93N PrrB may be impaired, at least in part, in its sensory or signal transduction function.

A ubiquinone binding site has been proposed to be located within the second periplasmic loop of the RegB transmembrane domain, and it has been proposed that binding of ubiquinone to this site inhibits RegB kinase activity (39). On the basis of these findings as well as the results presented above, we assumed that ubiquinone might not inhibit the kinase activity of the Q93N PrrB. To test this assumption in vitro, we purified Q93N PrrB from *E. coli* and determined the inhibitory effect of ubiquinone on PrrB autophosphorylation in vitro. As controls, we also included the WT form of PrrB (PrrB) and the truncated form of PrrB (C-PrrB), in which the 191 N-terminal amino acids are removed. As shown in Fig. 7, when purified PrrB (13 μM) was incubated in the presence of 250 μM ubiquinone, autophosphorylation of PrrB was completely abolished, which is consistent with the previous results by Swem et al. (39). In the presence of 250 μM ubiquinol in the autophosphorylation reaction mixture, autophosphorylation of PrrB was in part inhibited, but PrrB still retained autokinase activity. As a control of this experiment, the autophosphorylation assay of PrrB was performed in the presence of 10 mM DTT but in the absence of ubiquinol, since the ubiquinol-treated autophos-

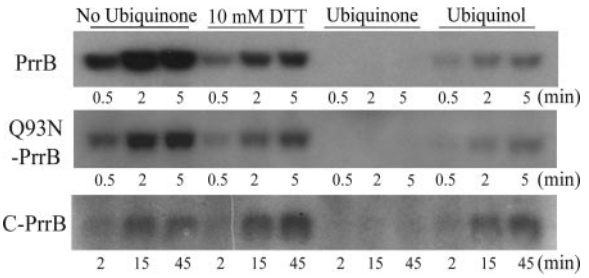

FIG. 7. Autophosphorylation of PrrB, C-PrrB, and the Q93N mutant form of PrrB in the presence of ubiquinone. The autophosphorylation reactions were performed by using 13 μM purified proteins in the presence or absence of ubiquinone (coenzyme Q1). The reaction mixtures containing DTT (10 mM), ubiquinone (250 μM), or ubiquinol (250 μM) were incubated at 30°C for 20 min, and the reaction was started by the addition of ATP. To generate ubiquinol from ubiquinone and to perform autophosphorylation assays in the presence of ubiquinol, DTT was added to the ubiquinone stock solution as well as the reaction mixture to a final concentration of 10 mM. The autophosphorylation reaction in the presence of 10 mM DTT was performed as a negative control reaction for the ubiquinol-treated reaction. At the time points indicated, samples (10 μl) were removed and added to 3 μl of loading buffer to stop the reaction. Because the autophosphorylation rate of C-PrrB was lower than that of PrrB, the phosphorylation reaction with C-PrrB was performed for longer time. The amount of protein phosphorylation was quantified by SDS-PAGE.

phorylation assay was performed in the reaction mixture containing 10 mM DTT to prevent the reoxidation of ubiquinol to ubiquinone. The presence of DTT in the reaction mixture led to a decrease in the autophosphorylation rate of PrrB, which contrasts with the results reported by Potter et al. (32). This difference can be explained by the fact that we included 20 mM β-mercaptoethanol in all buffers during the purification of PrrB so that purified PrrB was maintained in a reduced state without DTT treatment. The inhibition of PrrB autophosphorylation by ubiquinol might be a consequence of both the presence of DTT and the autooxidation of ubiquinol to ubiquinone during the 20 min of preincubation time. In the case of Q93N PrrB, its autophosphorylation was completely inhibited by ubiquinone as well, and the effect of DTT and ubiquinol on its autophosphorylation activity was similar to that of PrrB. Most significantly, the truncated form of PrrB (C-PrrB), which lacks the N-terminal transmembrane domain of PrrB, was also inhibited by ubiquinone but not by ubiquinol. This result most strongly reveals that the transmembrane domain of PrrB, which includes the proposed ubiquinone binding site, is not required for the inhibition of PrrB autophosphorylation by ubiquinone and throws into question any role for ubiquinone/ubiquinol in the regulation of PS gene expression through PrrB in *R. sphaeroides*, as originally proposed (39).

DISCUSSION

The catalytic subunit (CcoN or FixN) of the cbb_3 oxidase contains a low-spin heme *b* and a binuclear center consisting of a high-spin heme b_3 and Cu_B as the redox-related prosthetic groups (31, 41, 43). Seven conserved histidine residues of CcoN are involved in the coordination of the redox prosthetic groups and Mg^{2+} (Mn^{2+}) (8, 25, 41). H118 and H407 provide two axial ligands to the low-spin heme, while H405 provides an axial ligand to the high-spin heme (the numbering of *R. sphaeroides* CcoN). The Cu_B center is coordinated by H267, H317, and H318. Replacement of any of these histidine residues to alanine or valine by site-directed mutagenesis was demonstrated to lead to the loss of enzyme activity (25, 43). An additional five histidine residues (H214, H233, H303, H320, and H444) are also conserved in the CcoN (FixN) subunits of all known cbb_3 oxidases, except for those of *Helicobacter pylori* and *Campylobacter jejuni* (21, 37, 41). Interestingly, these same five histidines are not conserved in the catalytic subunits of other heme-copper superfamily oxidases, implying that some or all of them might be related to a function specific to the cbb_3 oxidase.

Using both the *R. sphaeroides* strains expressing the His_6-tagged H303A oxidase and the purified H303A oxidases, we have now been able to demonstrate unambiguously that the H303A mutation of the CcoN subunit of the cbb_3 oxidase affects neither its catalytic activity nor its assembly/stability of the cbb_3 oxidase in the membrane. This result is not consistent with previous findings showing that replacement of the corresponding histidine residue with valine in the FixN subunit of the *Bradyrhizobium japonicum* and the *R. capsulatus* enzymes leads to the loss of oxidase activity (29, 43). The disparity might result from the fact that the histidine residue was changed to valine in *B. japonicum* and *R. capsulatus* but to alanine in *R. sphaeroides* or there simply exists an intrinsic difference between these forms of the cbb_3 oxidase.

However, the most interesting phenotype displayed by *R. sphaeroides* expressing the H303A oxidase (H303A strain) is that when grown aerobically, the mutant strain produces photosynthetic spectral complexes accompanied by the derepression of PS gene expression levels, such as those for *puf* and *puc*. This "oxygen-insensitive spectral complex formation" does not occur in the *R. sphaeroides* strain synthesizing the WT oxidase (WT strain). Since cytochrome *c* oxidase activities detected in the H303A and WT strains are similar, spectral complex formation observed in the H303A strain grown under aerobic conditions cannot be a consequence of cellular redox changes caused by the impairment of the respiratory ETC but must result from a defective sensory (or signaling) function of the H303A oxidase. Note also that under aerobic respiratory conditions of growth, the aa_3 cytochrome *c* oxidase is fully functional, and the bulk of the reductant passes through this terminal oxidase on its way to the reduction of O_2. Taken together, these results fortify our previous conclusion that the cbb_3 oxidase per se functions as a redox sensor (25, 27) and leads us to conclude that the derepression of the PS genes observed in the H303A strain cannot result from changes in the redox state of the ubiquinone/ubiquinol pool. The H303A mutation might place the cbb_3 oxidase into a conformation that causes it to malfunction in the generation of the intrinsic inhibitory signal, resulting in the apparent diminution of PrrB kinase activity in the presence of O_2.

Through sequence analysis and homology modeling of the catalytic subunits of the cbb_3 oxidases and other heme-copper family oxidases, it was suggested that H303 might be involved in the formation of the K channel involved in proton transfer and that the CcoQ subunit might be located in the vicinity of transmembrane helix 7 of CcoN where H303 resides (37). If this were true, the H303A mutation could affect proton pump-

ing through the K channel and assembly of CcoQ into the cbb_3 core enzyme complex composed of CcoN, CcoO, and CcoP. Because blocking of the K channel is known to hinder the reductive phase of O_2 reduction (15), the H303A oxidase appears not to be impaired in proton pumping as judged by its normal catalytic activity. The phenotype of a *ccoQ* in-frame deletion mutant strain of *R. sphaeroides* was reported to be similar to that of the H303A strain with regard to both normal cytochrome *c* oxidase activity under anaerobic conditions and oxygen-insensitive formation of the spectral complexes (22). Subunit abundance and cbb_3 oxidase activity in the *ccoQ* deletion mutant were shown to be significantly reduced under aerobic growth conditions compared with measurements of the WT strain grown under the same conditions (24). We observed that the levels of the CcoN and CcoP subunits in the membrane fractions of CBB3Δ [pUIH303A] grown under aerobic conditions are similar to those of CBB3Δ [pUI2803NHIS] grown under the same conditions, which indicates that the phenotype observed in the H303A strain does not result from the incorrect conformation or assembly of CcoQ in the enzyme complex.

Besides the cbb_3 oxidase, the redox state of the ubiquinone/ubiquinol pool was suggested to influence RegB (PrrB) kinase activity (39). Site-directed mutagenesis of the second periplasmic loop of the PrrB transmembrane domain led us to identify that the Q93N mutation results in spectral complex formation and derepression of *puf* operon expression in the mutant strain grown under aerobic conditions. Based on these observations, we concluded that the Q93N mutant form of PrrB is impaired in its signal sensory or signal transduction function. If the signal is through ubiquinone binding, as proposed by Swem et al. (39), the autophosphorylation rate of Q93N PrrB is not expected to be inhibited by ubiquinone. Yet, ubiquinone treatment led to the inhibition of autophosphorylation of Q93N PrrB. Quite unexpectedly from using an important control reaction, the inhibitory effect of ubiquinone on the autophosphorylation rate was also observed for the truncated form of PrrB lacking the N-terminal transmembrane domain and, thus, not possessing the proposed ubiquinone binding site. These results can imply only that the cytoplasmic kinase domain of PrrB is responsible for the inhibition of kinase activity in the presence of ubiquinone. To determine whether the inhibitory effect of ubiquinone is generally exerted on the autophosphorylation rate of all histidine kinases, we performed an identical autophosphorylation assay on the purified DevS histidine kinase of *Mycobacterium smegmatis* in the presence or absence of 250 μM ubiquinone as well as menaquinone (vitamin K_1). Neither ubiquinone nor menaquinone affected the autophosphorylation rate of DevS (data not shown), indicating that the ubiquinone effect cannot be applied to all histidine kinases.

Interestingly, the so-called H box of the PrrB kinase domain contains a sequence (AAAAHELGTP [the underlined H indicates the autophosphorylatable histidine]) that shows similarity to the proposed quinone binding motif found in the quinone binding sites of bacterial reaction centers, bc_1 complexes, and NADH dehydrogenase complexes [aliphatic amino acid-$(X)_3$-H-$(X)_{2,3}$-(L/T/S)] (7). The DevS histidine kinase, whose autophosphorylaton rate is not affected by ubiquinone, does not contain such a ubiquinone binding motif in its H box. At present it is, however, uncertain as to whether the putative quinone binding motif present in the H box of PrrB is responsible for ubiquinone binding and inhibition of PrrB autophosphorylation.

The mechanism(s) by which the activity of the PrrB histidine kinase is controlled in response of redox changes cannot be explained by either the ubiquinone binding model or the redox-active cysteine model for the following reasons. (i) Under aerobic growth conditions, PS gene expression is not derepressed in the aa_3 cytochrome *c* oxidase mutant of *R. sphaeroides* in which the major aa_3 cytochrome *c* oxidase is inactivated, while inactivation of the cbb_3 cytochrome *c* oxidase results in PS gene derepression under aerobic conditions. In the aa_3 mutant strain, the bulk of the reductant passing through the aerobic respiratory ETC is altered and it would be anticipated that such an alteration would increase the relative ubiquinol to ubiquinone abundance and, thus, turn on PS gene expression (25). (ii) Overexpression of the *ccoNOQP* operon in *R. sphaeroides* leads to a decrease in PS gene expression under anaerobic photosynthetic growth conditions where the substrate of the cbb_3 oxidase (O_2) is absent (22). It is unlikely that such an effect could influence the relative abundance of ubiquinone/ubiquinol. (iii) Overexpression of *prrB* in *R. sphaeroides* brings about spectral complex formation even under aerobic conditions (26). Similarly, it is difficult to imagine any plausible effect on the ubiquinone/ubiquinol pools. (iv) In the absence of the cbb_3 complex under anaerobic conditions, PS gene expression is increased (20). (v) Finally, the PrrBL78P mutant, having an intact proposed ubiquinone binding sequence, shows marked derepression of PS gene expression aerobically (5). These observations can be understood only if the cbb_3 cytochrome *c* oxidase must be involved in the redox-responsive control of PrrB activity. However, we still do not know the underlying mechanism by which the cbb_3 oxidase communicates with the PrrB histidine kinase to control its activity, and this is the goal of future study to reveal this mechanism. Nonetheless, the role of H303 raises several interesting possibilities.

ACKNOWLEDGMENTS

This work was supported by a Korea Research Foundation grant (KRF-2004-015-C00488) to Jeong-Il Oh and by grant USPHS GM15590 to Samuel Kaplan.

REFERENCES

1. **Comolli, J. C., A. J. Carl, C. Hall, and T. Donohue.** 2002. Transcriptional activation of the *Rhodobacter sphaeroides* cytochrome c_2 gene P2 promoter by the response regulator PrrA. J. Bacteriol. **184:**390–399.
2. **Davis, J., T. J. Donohue, and S. Kaplan.** 1988. Construction, characterization, and complementation of a Puf$^-$ mutant of *Rhodobacter sphaeroides*. J. Bacteriol. **170:**320–329.
3. **Dubbs, J. M., T. H. Bird, C. E. Bauer, and F. R. Tabita.** 2000. Interaction of CbbR and RegA* transcription regulators with the *Rhodobacter sphaeroides* cbb_I promoter-operator region. J. Biol. Chem. **275:**19224–19230.
4. **Eraso, J. M., and S. Kaplan.** 1996. Complex regulatory activities associated with the histidine kinase PrrB in expression of photosynthesis genes in *Rhodobacter sphaeroides* 2.4.1. J. Bacteriol. **178:**7037–7046.
5. **Eraso, J. M., and S. Kaplan.** 1995. Oxygen-insensitive synthesis of the photosynthetic membranes of *Rhodobacter sphaeroides*: a mutant histidine kinase. J. Bacteriol. **177:**2695–2706.
6. **Eraso, J. M., and S. Kaplan.** 1994. *prrA*, a putative response regulator involved in oxygen regulation of photosynthesis gene expression in *Rhodobacter sphaeroides*. J. Bacteriol. **176:**32–43.
7. **Fisher, N., and P. R. Rich.** 2000. A motif for quinone binding sites in respiratory and photosynthetic systems. J. Mol. Biol. **296:**1153–1162.
8. **García-Horsman, J. A., B. Barquera, J. Rumbley, J. Ma, and R. B. Gennis.** 1994. The superfamily of heme-copper respiratory oxidases. J. Bacteriol. **176:**5587–5600.

9. **Jessee, J.** 1986. New subcloning efficiency competent cells: $>1 \times 10^6$ transformants/μg. Focus **8:**9.
10. **Joshi, H. M., and F. R. Tabita.** 1996. A global two-component signal transduction system that integrates the control of photosynthesis, carbon dioxide assimilation, and nitrogen fixation. Proc. Natl. Acad. Sci. USA **93:**14515–14520.
11. **Kaplan, S., J. Eraso, and J. H. Roh.** 2005. Interacting regulatory networks in the facultative photosynthetic bacterium, Rhodobacter sphaeroides 2.4.1. Biochem. Soc. Trans. **33:**51–55.
12. **Keen, N. T., S. Tamaki, D. Kobayashi, and D. Trollinger.** 1988. Improved broad-host-range plasmids for DNA cloning in gram-negative bacteria. Gene **70:**191–197.
13. **Kiley, P. J., and S. Kaplan.** 1988. Molecular genetics of photosynthetic membrane biosynthesis in *Rhodobacter sphaeroides*. Microbiol. Rev. **52:** 50–69.
14. **Kim, Y. J., I. J. Ko, and J. I. Oh.** 2006. Identification of amino acids involved in the sensory function of the PrrB histidine kinase by site-directed mutagenesis. Korean J. Life Sci. **16:**485–492.
15. **Konstantinov, A. A., S. Siletsky, D. Mitchell, A. Kaulen, and R. B. Gennis.** 1997. The roles of the two proton input channels in cytochrome c oxidase from *Rhodobacter sphaeroides* probed by the effects of site-directed mutations on time-resolved electrogenic intraprotein proton transfer. Proc. Natl. Acad. Sci. USA **94:**9085–9090.
16. **Laemmli, U. K.** 1970. Cleavage of structural proteins during the assembly of the head of bacteriophage T_4. Nature **227:**680–685.
17. **Laratta, W. P., P. S. Choi, I. E. Tosques, and J. P. Shapleigh.** 2002. Involvement of the PrrB/PrrA two-component system in nitrite respiration in *Rhodobacter sphaeroides* 2.4.3: evidence for transcriptional regulation. J. Bacteriol. **184:**3521–3529.
18. **Lee, J. K., and S. Kaplan.** 1992. *cis*-acting regulatory elements involved in oxygen and light control of *puc* operon transcription in *Rhodobacter sphaeroides*. J. Bacteriol. **174:**1146–1157.
19. **Mouncey, N. J., and S. Kaplan.** 1998. Redox-dependent gene regulation in *Rhodobacter sphaeroides* $2.4.1^T$: effects on dimethyl sulfoxide reductase (*dor*) gene expression. J. Bacteriol. **180:**5612–5618.
20. **O'Gara, J. P., J. M. Eraso, and S. Kaplan.** 1998. A redox-responsive pathway for aerobic regulation of photosynthesis gene expression in *Rhodobacter sphaeroides* 2.4.1. J. Bacteriol. **180:**4044–4050.
21. **Oh, J. I.** 2006. Effect of mutations of five conserved histidine residues in the catalytic subunit of the cbb_3 cytochrome c oxidase on its function. J. Microbiol. **44:**284–292.
22. **Oh, J. I., and S. Kaplan.** 1999. The cbb_3 terminal oxidase of *Rhodobacter sphaeroides* 2.4.1: structural and functional implications for the regulation of spectral complex formation. Biochemistry **38:**2688–2696.
23. **Oh, J. I., and S. Kaplan.** 2001. Generalized approach to the regulation and integration of gene expression. Mol. Microbiol. **39:**1116–1123.
24. **Oh, J. I., and S. Kaplan.** 2002. Oxygen adaptation: the role of the CcoQ subunit of the cbb_3 cytochrome c oxidase of *Rhodobacter sphaeroides* 2.4.1. J. Biol. Chem. **277:**16220–16228.
25. **Oh, J. I., and S. Kaplan.** 2000. Redox signaling: globalization of gene expression. EMBO J. **19:**4237–4247.
26. **Oh, J. I., I. J. Ko, and S. Kaplan.** 2001. The default state of the membrane-localized histidine kinase PrrB of *Rhodobacter sphaeroides* 2.4.1 is in the kinase-positive mode. J. Bacteriol. **183:**6807–6814.
27. **Oh, J. I., I. J. Ko, and S. Kaplan.** 2004. Reconstitution of the *Rhodobacter sphaeroides* cbb_3-PrrBA signal transduction pathway in vitro. Biochemistry **43:**7915–7923.
28. **Ouchane, S., and S. Kaplan.** 1999. Topological analysis of the membrane-localized redox-responsive sensor kinase PrrB from *Rhodobacter sphaeroides* 2.4.1. J. Biol. Chem. **274:**17290–17296.
29. **Öztürk, M., and S. Mandaci.** 2 December 2006, posting date. Two conserved non-canonical histidines are essential for activity of the cbb_3-type oxidase in *Rhodobacter capsulatus*: non-canonical histidines are essential for cbb_3-type oxidase activity in *R. capsulatus*. Mol. Biol. Rep. doi: 10.1007/s11033-006-9031-9.
30. **Parson, W. W.** 1975. Quinones as secondary electron acceptors. *In* R. K. Clayton and W. R. Sistrom (ed.), The photosynthetic bacteria. Plenum Publishing Corp., New York, NY.
31. **Pitcher, R. S., and N. J. Watmough.** 2004. The bacterial cytochrome cbb_3 oxidases. Biochim. Biophys. Acta **1655:**388–399.
32. **Potter, C. A., E. L. Jeong, M. P. Williamson, P. J. Henderson, and M. K. Phillips-Jones.** 2006. Redox-responsive in vitro modulation of the signalling state of the isolated PrrB sensor kinase of *Rhodobacter sphaeroides* NCIB 8253. FEBS Lett. **580:**3206–3210.
33. **Potter, C. A., A. Ward, C. Laguri, M. P. Williamson, P. J. Henderson, and M. K. Phillips-Jones.** 2002. Expression, purification and characterisation of full-length histidine protein kinase RegB from *Rhodobacter sphaeroides*. J. Mol. Biol. **320:**201–213.
34. **Qian, Y., and F. R. Tabita.** 1996. A global signal transduction system regulates aerobic and anaerobic CO_2 fixation in *Rhodobacter sphaeroides*. J. Bacteriol. **178:**12–18.
35. **Roh, J. H., W. E. Smith, and S. Kaplan.** 2004. Effects of oxygen and light intensity on transcriptome expression in *Rhodobacter sphaeroides* 2.4.1. Redox active gene expression profile. J. Biol. Chem. **279:**9146–9155.
36. **Sambrook, J., E. F. Fritsch, and T. Maniatis.** 1989. Molecular cloning: a laboratory manual, 2nd ed. Cold Spring Harbor Laboratory Press, Cold Spring Harbor, NY.
37. **Sharma, V., A. Puustinen, M. Wikstrom, and L. Laakkonen.** 2006. Sequence analysis of the cbb_3 oxidases and an atomic model for the *Rhodobacter sphaeroides* enzyme. Biochemistry **45:**5754–5765.
38. **Simon, R., U. Priefer, and A. Puhler.** 1983. A broad host range mobilization system for in vivo genetic engineering: transposon mutagenesis in gram-negative bacteria. Nat. Biotechnol. **1:**784–791.
39. **Swem, L. R., X. Gong, C. A. Yu, and C. E. Bauer.** 2006. Identification of a ubiquinone binding site that affects autophosphorylation of the sensor kinase RegB. J. Biol. Chem. **281:**6768–6775.
40. **Swem, L. R., B. J. Kraft, D. L. Swem, A. T. Setterdahl, S. Masuda, D. B. Knaff, J. M. Zaleski, and C. E. Bauer.** 2003. Signal transduction by the global regulator RegB is mediated by a redox-active cysteine. EMBO J. **22:**4699–4708.
41. **Toledo-Cuevas, M., B. Barquera, R. B. Gennis, M. Wikstrom, and J. A. Garcia-Horsman.** 1998. The cbb_3-type cytochrome c oxidase from *Rhodobacter sphaeroides*, a proton-pumping heme-copper oxidase. Biochim. Biophys. Acta. **1365:** 421–434.
42. **van Neil, C. B.** 1944. The culture, general physiology, morphology, and classification of the non-sulfur purple and brown bacteria. Bacteriol. Rev. **8:**1–118.
43. **Zufferey, R., E. Arslan, L. Thony-Meyer, and H. Hennecke.** 1998. How replacements of the 12 conserved histidines of subunit I affect assembly, cofactor binding, and enzymatic activity of the *Bradyrhizobium japonicum* cbb_3-type oxidase. J. Biol. Chem. **273:**6452–6459.